Energy for Sustainable Development 25 (2015) 8–16

Contents lists available at ScienceDirect

Energy for Sustainable Development

Evaluation of power generation from thermoelectric cooler at normal and low-temperature cooling conditions

Wei-Hsin Chen [a,*], Chen-Yeh Liao [b], Chien-Chang Wang [b], Chen-I Hung [b]

[a] Department of Aeronautics and Astronautics, National Cheng Kung University, Tainan 701, Taiwan, ROC
[b] Department of Mechanical Engineering, National Cheng Kung University, Tainan 701, Taiwan, ROC

ARTICLE INFO

Article history:
Received 14 December 2013
Revised 16 December 2014
Accepted 16 December 2014
Available online xxxx

Keywords:
Thermoelectric cooler (TEC)
Seebeck coefficient
Power generation
Numerical prediction
Low-temperature and normal cooling

ABSTRACT

Three different methods for predicting the Seebeck coefficient and power generation of a commercial available thermoelectric cooler (TEC) module are used and compared to the experimental data. Method 1 and 2 are developed based on mathematical models and Method 3 is established in terms of experimental measurements. Method 3 considers the effect of cooling condition, whereas Method 1 and 2 don't. Two different temperatures at the cold side of the TEC module are also considered to account for the influence of cooling condition on the performance of the TEC. The power generation of the TEC module with low-temperature cooling is at least 5% higher than that with normal cooling. Method 3 gives the best prediction in open circuit voltage and power generation. Basically, the three methods are able to evaluate the properties and performance of a TEC easily, thereby providing useful tools for designing and constructing a TE generation system.

© 2014 International Energy Initiative. Published by Elsevier Inc. All rights reserved.

Introduction

Thermoelectric coolers (TECs) are one of the coolers used for refrigeration. They are based on the Peltier effect (Gurevich and Logvinov, 2005; Meng et al., 2014a; Wang et al., 2012a; Chen et al., 2014a). When the electric power is applied, heat energy will be absorbed on one side of the TEC and dissipated on the other side so as to achieve cooling purpose. The cooling performances of commercial TECs can be evaluated by several parameters, such as the maximum temperature difference (ΔT_{max}), the maximum absorbed heat ($Q_{c,max}$), the coefficient of performance (*COP*), and the figure of merit (Z). In general, the first two parameters, ΔT_{max} and $Q_{c,max}$, of the commercial TECs are provided by manufacturers. The maximum temperature difference (ΔT_{max}) across the TEC is identified when the absorbed heat or cooling power is equal to zero, whereas the maximum absorbed heat ($Q_{c,max}$) develops when ΔT is zero. *COP* is the ratio of absorbed heat to applied electric power, and Z is defined by Ioffe (1957), Mahan (1989), Abramzon (2007) and Wang et al. (2014)

$$Z = \frac{a^2}{\rho_e} \tag{1}$$

where α, ρ_e, and k are the Seebeck coefficient (V K^{-1}), electrical resistivity (Ω m), and thermal conductivity (W m^{-1} K^{-1}), respectively. A higher value of *COP* or Z value leads to a better performance of TEC.

Compared with other coolers, TECs possess numerous benefits, such as direct electric energy conversion, compact structure without moving parts causing vibration or noise, no refrigerants, high reliability, low maintenance fee, and easy control (Simons et al., 2005; Huang et al., 2005; Wang et al., 2012b). Consequently, much research has been carried out in recent years (Wu and Hung, 2009; Martinez et al., 2011; Chen et al., 2012a). Among the related research, the concept of TECs for power generation was developed by Min and Rowe (1998). They noted that commercially available TECs could also be used to recover low-temperature waste heat and generate power but not just used for refrigeration. Waste heat can be found extensively in industrial processes (Chen et al., 2005; Chen and Syu, 2011) and no cost is required when it is reused. Therefore, TECs are a potential device to fulfill electricity generation from waste heat. Some researchers have employed TECs for thermoelectric power generation (Maneewan and Chindaruksa, 2009; Chen et al., 2012b). This conversion process by transforming heat energy into electricity is based on the Seebeck effect (Meng et al., 2014b; Meng et al., 2015; Chen et al., 2014b). The conversion efficiency of TECs is relatively low, typically around 5% (Riffat and Ma, 2003). Nevertheless, this drawback can be resolved when the heat energy comes from waste heat (Riffat and Ma, 2003; Bell, 2008). Besides, compared with TE generators (TEGs) originally designed for TE power generation,

* Corresponding author. Tel.: +886 6 2004456; fax: +886 6 2389940.
E-mail address: weihsinchen@gmail.com (W.-H. Chen).

http://dx.doi.org/10.1016/j.esd.2014.12.004
0973-0826/© 2014 International Energy Initiative. Published by Elsevier Inc. All rights reserved.

Nomenclature

A	cross-sectional area of thermoelectric element (m^2)
B	constant (V)
C	constant ($V\ K^{-1}$)
D	constant (depends on the used data)
COP	coefficient of performance (dimensionless)
I	electric current (A)
k	thermal conductivity ($W\ m^{-1}\ K^{-1}$)
L	length of thermoelectric element (m)
N	number of thermoelectric pairs (dimensionless)
P	power (W)
Q_c	cooling power (W)
T	temperature (°C)
T_w	temperature of water in the tank (°C)
V	voltage (V)
Z	thermoelectric figure-of-merit (K^{-1})

Greek letters

a	Seebeck coefficient ($V\ K^{-1}$)
ΔT	temperature difference across the thermoelectric module (°C)
ρ_e	electrical resistivity (Ω m)

Subscript

c	cold side
H	heating surface
h	hot side
l	load
oc	open circuit
out	output
max	maximum
w	water

TECs, which have lower cost, are more suitable to be used for low-temperature waste heat recovery (Chen et al., 2012b).

However, unlike the cooling performance, the parameters to access the power generation of TECs are hardly found in the datasheet provided by manufacturers. Therefore, several researchers have explored the procedure to obtain the interior parameters or material properties of TECs. Huang et al. (2000) utilized fully automatic testing instruments to acquire the properties of TECs. Luo (2008) presented a mathematical method to estimate the characteristics of TECs. Although the parameters obtained from the experiment are more precise than those from the mathematical method to predict the performances of TECs in a real situation, the automatic testing instruments are not accessible for users. Hence, the mathematical method presented by Luo (2008) is more feasible for users to select the appropriate TECs (Palacios et al., 2009). Similar research can be found for TEGs. Woo and Lee (2003) conducted an experiment to find the relationship between the generated voltage and temperature difference across a TEG. Hsu et al. (2011) also constructed an experimental system and proposed the concept of effective Seebeck coefficient to discuss the inconsistency between the theoretical analyses and measured results.

This study is intended to predict the performances of a TEC obtained using various mathematical models and compare with the experimental measurements. An experimental system is constructed to obtain the power generation of the TEC at certain conditions. Particular attention is paid to the performances of the TEC at two different cooling situations with one the low-temperature cooling condition ($T_w \cong 1$ °C) and the other the normal cooling condition ($T_w \cong 30$ °C). The mathematical models presented by Luo (2008) and Woo and Lee (2003) will be used to calculate the parameters and power generation of the TEC for comparison.

Methodology

Mathematical model

For TEC users, there are two simple ways to estimate the properties of TEC (Luo, 2008). When these methods are adopted, some assumptions have to be made. They include: (1) the steady state running; (2) no heat loss from convection and radiation; (3) no contact resistance; (4) the equivalent scales of p- and n-type elements in each TE pair; and (5) no temperature dependence of material properties. In addition, the hot side temperature of the TEC (T_h), the number of the TE pairs inside the TEC (N), and the length (L) and cross-area (A) of the element have to be known. A TE pair is composed of a p-type element, an n-type element, and conductors to connect the two elements, as shown in Fig. 1. Four parameters of ΔT_{max}, $Q_{c,max}$, I_{max}, and V_{max} are available in the datasheet which are used for the two methods. ΔT_{max} and $Q_{c,max}$ have been illustrated earlier; I_{max} is the electric current resulting in ΔT_{max}, and V_{max} is the voltage applied on the TEC at $I = I_{max}$ and $\Delta T = \Delta T_{max}$. Method 1 uses three parameters of ΔT_{max}, I_{max}, and V_{max} to predict the properties of the TEC as the following (Luo, 2008).

$$\alpha = \frac{1}{2N} \cdot \frac{V_{max}}{T_h} \tag{1}$$

$$\rho_e = \frac{A}{2NL} \cdot \frac{V_{max}(T_h - \Delta T_{max})}{I_{max} T_h} \tag{2}$$

$$k = \frac{L}{2NA} \cdot \frac{I_{max} V_{max}(T_h - \Delta T_{max})}{T_h \Delta T_{max}}. \tag{3}$$

Method 2 uses $Q_{c,max}$, I_{max}, and V_{max} to predict the properties of the TEC as follows (Luo, 2008).

$$\alpha = \frac{1}{N} \cdot \frac{Q_{c,max}}{I_{max}(T_h + \Delta T_{max})} \tag{4}$$

$$\rho_e = \frac{A}{NL} \cdot \frac{Q_{c,max}(T_h - \Delta T_{max})}{I_{max}^2 (T_h + \Delta T_{max})} \tag{5}$$

$$k = \frac{L}{2NA} \cdot \frac{Q_{c,max}(T_h - \Delta T_{max})}{\Delta T_{max}(T_h + \Delta T_{max})}. \tag{6}$$

After getting the material properties, the open circuit voltage and output power of the TEC for the two methods can be obtained by

$$V_{oc} = \alpha \Delta T \tag{7}$$

$$P_{out} = (\alpha \Delta T - IR)I \tag{8}$$

where R is the internal resistance of the TEC and it can be measured or calculated by the following equation

$$R = 2N\rho_e \frac{L}{A}. \tag{9}$$

The Seebeck coefficient of the TEC can also be obtained from the work of Woo and Lee (2003). Although they used the experimental results to find the relationship between the open circuit voltage (V_{oc}) and the temperature difference (ΔT), the experimental system was simpler than that in the work of Huang et al. (2000). Therefore, the work of Woo and Lee (2003) is useful for users who have simpler equipment and it is referred to as Method 3 herein. In their work, the linear

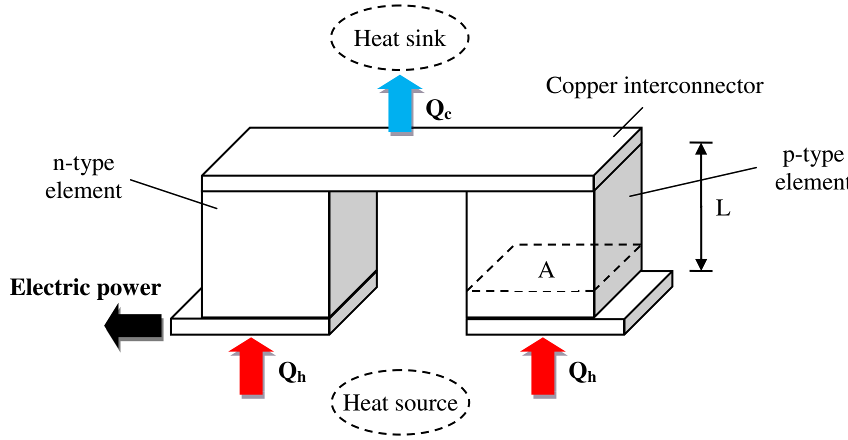

Fig. 1. The schematic of Seebeck effect of a TE pair.

relationship between the V_{oc} and ΔT is given as the following form (Woo and Lee, 2003)

$$V_{oc} = B + C\Delta T \tag{10}$$

where B and C are constants. In this method, the Seebeck coefficient is calculated by neglecting the constant B and using the constant C as follows

$$\alpha \approx \frac{C}{2N} = \frac{1}{2N} \cdot \frac{V_{oc}}{\Delta T}. \tag{11}$$

Then, the output power of the TEC is predicted by Eq. (8) where R is measured from the experiment.

As shown above, the power generation of the TEC can be predicted as long as the Seebeck coefficient and the temperature difference are known. Therefore, this study is intended to use the given temperature differences and the calculated Seebeck coefficients to estimate the power generation of the TEC.

Experimental system

To compare with the results obtained from the aforementioned methods, an experiment system was developed. The experimental system, as shown in Fig. 2, was made up of a heater (MS41N), an aluminum plate, a TEC module, a heat sink with the cold fluid loop, a compressive load, an electronic load, and a data acquisition unit. The heater was built by a cartridge heater which was situated in an aluminum block. The aluminum plate was used to make temperature measurement easier at the hot side. The size and characteristics of the TEC module (TECCP-24-002) adopted for study are listed in Table 1. The aluminum plate and the heat sink covered by thermal grease were attached to the TEC. The cold fluid loop comprised a pump, a tank (5 L), a radiator with two axial fans, a flow meter (RRI-010/050), pipes, and a coolant (water or ice water).

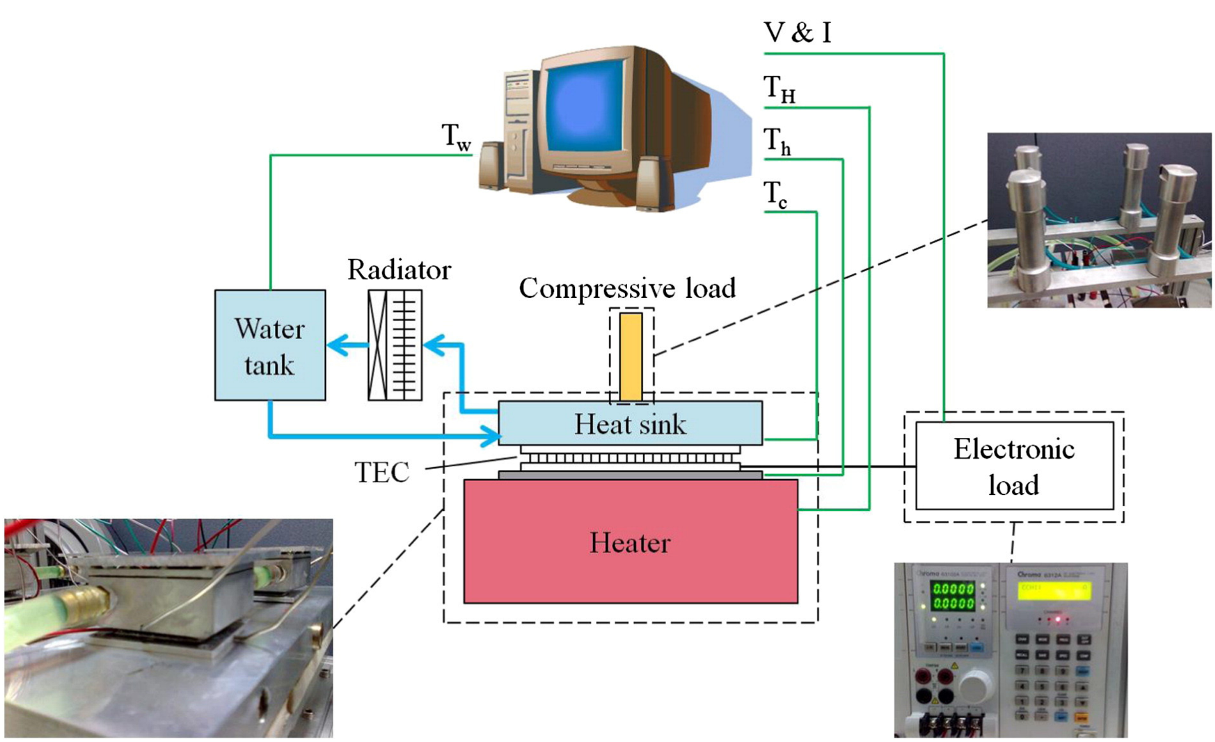

Fig. 2. The schematic of the experimental system.

Table 1
Physical sizes and characteristics of the tested thermoelectric cooling (TEC) module.

Module	TECCP-24-002
No. of TE pairs (—)	127
Length, width, height (mm)	40, 40, 3.3
I_{max} (A)	10
V_{max} (V)	15.4
$Q_{c,max}$ (W)	88.9
ΔT_{max} (°C)	67

The compressive load attached to the heat sink was used to reduce the thermal contact resistance. The electronic load (Chromas 6312A and 63102A) was employed as the external load. The data acquisition unit included a computer and three PLC modules; type numbers of the PLC modules are FBs-TC16, FBs-6AD, and FBs-20MA. In addition, K-type thermocouples were used to measure the hot side (T_h) and cold side (T_c) temperatures of the TEC and the temperature of water in the tank (T_w).

Experimental procedure

In the experiments, the heater with temperature controller (MS41N) continuously supplied thermal energy to the TEC, and the temperature of the heater was adjusted to reach the desired temperature difference across the TEC. The upper limit of heating temperature was about 200 °C since it was the maximum operating temperature of the TEC. The TEC then converted thermal energy to electricity, as shown in Fig. 1. The residual thermal energy at the cold side was removed by the heat sink and cold fluid loop. At the cooling side, two different coolants were taken into account. One was the mixture of water and ice which could make the temperature of the coolant around 1 °C; the other was water alone whose temperature was maintained at around 30 °C. When the first coolant was used, it was referred to as the low-temperature cooling condition, whereas it was referred to as the normal cooling condition for the second coolant. The flow rate of the coolants was fixed at 1.0 L min^{-1} and it was controlled by the pump and measured by the flowmeter. The compressive load attached to the heat sinks was set at 60 psi which was sufficiently large to diminish the gaps and thermal contact resistances of the interfaces. The electricity generated by the TEC was measured by the electronic load. All measured data, including the temperature difference across the TEC, the open circuit voltage, and the output power of the TEC, were recorded by the data acquisition unit for further analysis.

The resolutions of the flow meter, electronic load, and thermocouples were 0.01 L min^{-1}, 1.25 mV, and 0.1 °C, respectively. From the concepts of Kline (1985) and Coleman and Steele (1989), the uncertainty of the experiments was smaller than 5% so that the experimental results were reliable. Moreover, each case has been tested at least twice and the repeatability of the experiments has been ensured.

Results and discussion

Effect of cooling condition

First of all, the two different coolants are used to explore the effect of cooling conditions on the power generation of the TEC. The distributions

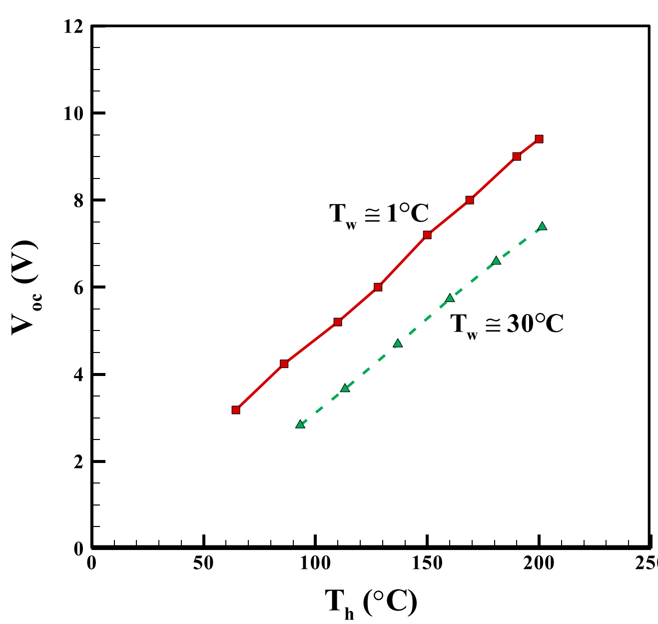

Fig. 3. Distributions of open circuit voltage (V_{oc}) versus hot side temperature (T_h) at two different cooling conditions.

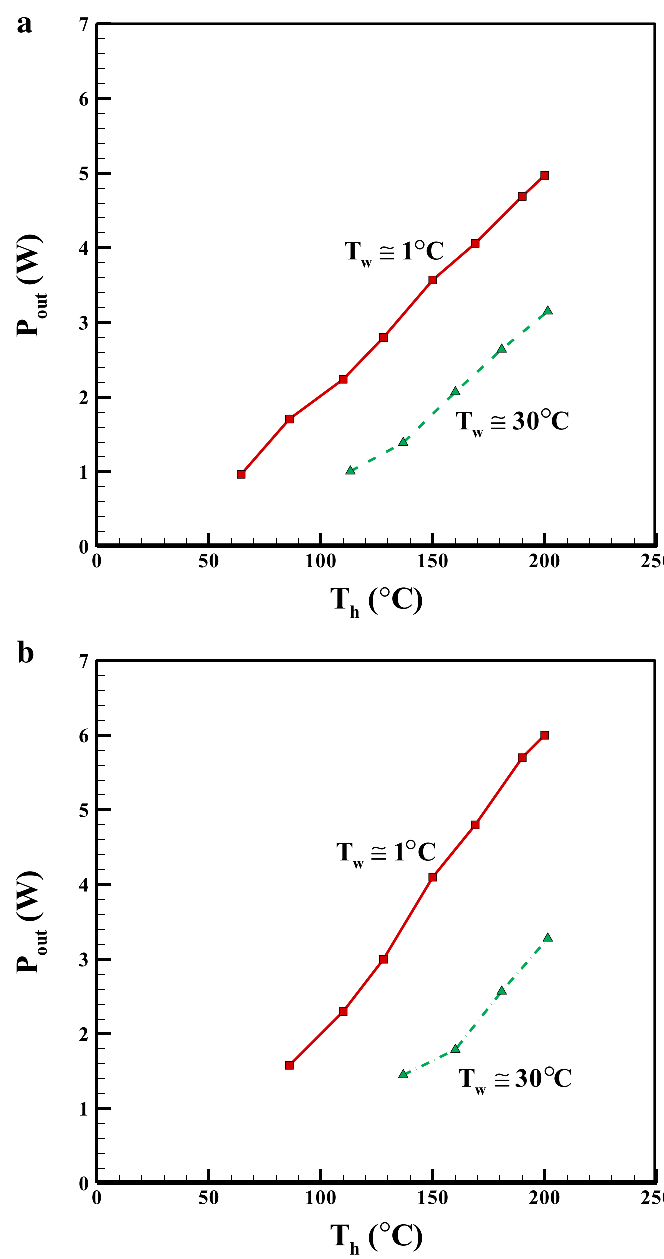

Fig. 4. Distributions of output power (P_{out}) versus hot side temperature at (a) I = 0.7 A and (b) I = 1.0 A under two different cooling conditions.

of open circuit voltage with increasing hot side temperature at the two cooling conditions are shown in Fig. 3. It is clear that the curve of the open circuit voltage at the low-temperature cooling condition is higher than that at the normal cooling condition. The profiles of output power with increasing hot side temperature at the electric currents of 0.7 and 1.0 A are plotted in Fig. 4a and b, respectively. The profiles of output power at the low-temperature cooling condition are also higher than the other one, regardless of which electric current is used. This can be explained by the temperature difference across the TEC becomes larger when the hot side temperature is fixed and the cold side has a lower temperature. In general, the larger the temperature difference, the better the TE power generation.

To proceed farther into an analysis of the TEC performance at the two cooling conditions, the distributions of the open circuit voltage and output power of the TEC versus the temperature difference across the TEC are plotted in Figs. 5 and 6, respectively. Overall, when the temperature difference is the same, the power generation of the TEC at the low-temperature cooling condition is higher than that at the normal one of at least 5%. This is due to the temperature dependence of the material properties of the TEC. Specifically, the material properties of the TEC will affect the value of $Z(=\alpha^2/\rho_e\, k)$ and thereby the performance of the TEC at different cooling conditions. From Figs. 5 and 6, it is recognized that the Z value of the TEC is higher at the low-temperature cooling condition. Therefore, the TEC generates more power when the coolant temperature is lower.

Furthermore, the improvement of the performance of the TEC in accordance with the variation of the open circuit voltage or output power at the two cooling conditions are defined as the following

$$\text{Improvement of performance } (\%) = \frac{\left|D_{\text{low-temperature}} - D_{\text{normal}}\right|}{D_{\text{normal}}} \times 100 \tag{12}$$

where D denotes the open circuit voltage or the output power. The distributions of the improvement are presented in Fig. 7. For the open circuit voltage, its improvement is between 4.7 and 15.8% (Fig. 7a), where the maximum and the minimum improvements occur at the temperature differences of 120 and 80 °C, respectively. With regard to the output power, its improvement can be lifted up to 69.4 (at ΔT = 80 °C) and 58.6% (at ΔT = 120 °C) when the electric currents are 0.7 and 1.0 A, respectively. These results clearly reflect that the operation of the TEC with low-temperature cooling is able to enhance its performance.

Calculations of Seebeck coefficient and power generation

Subsequently, the properties of the TEC are evaluated from the aforementioned three methods and they are further used to predict the power generation of the TEC. The parameters required in Method 1 and Method 2 are given in Table 1. Considering Method 1, the material properties are calculated from Eqs. (1)–(3) and the Seebeck coefficient from the calculation is around 2.021×10^{-4} V K^{-1}. Accordingly, the values of output power of the TEC at various electric currents can be predicted from Eqs. (7)–(9) where the estimated internal resistance is around 1.20 Ω. Alternatively, Eqs (4)–(9) are used in Method 2. The calculated Seebeck coefficient and internal resistance are around

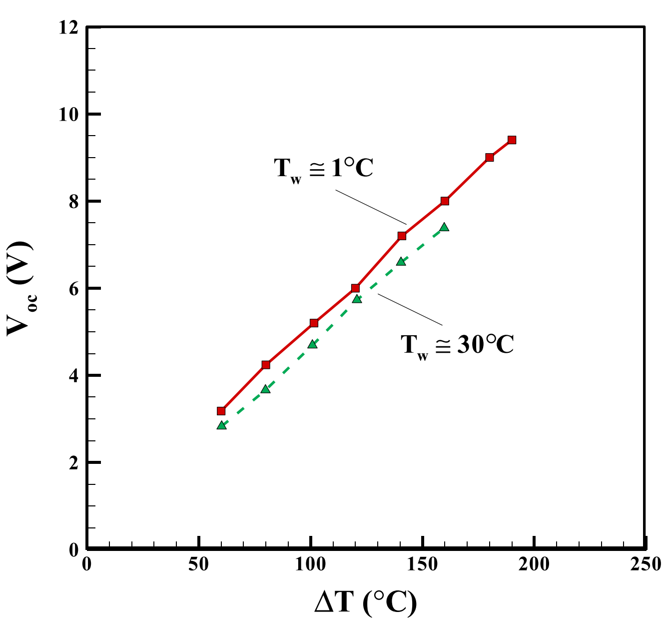

Fig. 5. Distributions of open circuit voltage versus temperature difference (ΔT) at two different cooling conditions.

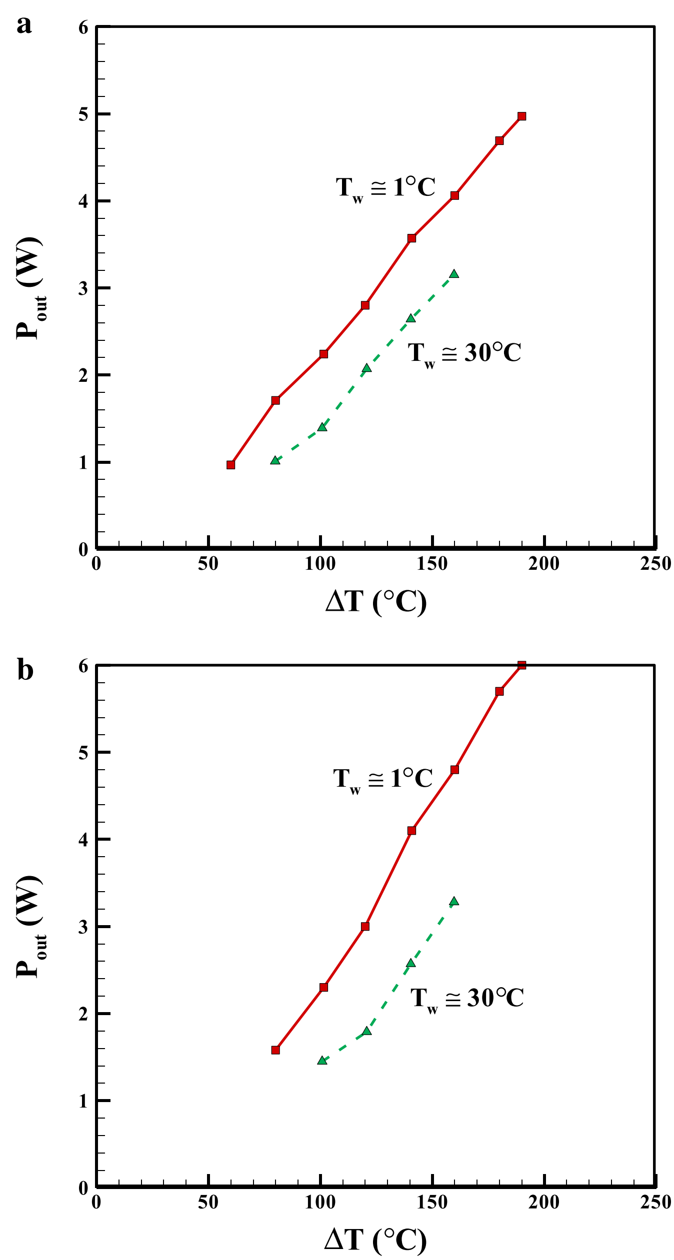

Fig. 6. Distributions of output power versus temperature difference at (a) I = 0.7 A and (b) I = 1.0 A under two different cooling conditions.

1.907×10^{-4} V K^{-1} and 0.97 Ω, respectively. In regard to Method 3, the evaluation is based on the experimental data. The data of the open circuit voltage of the TEC at various temperature differences have been displayed in Fig. 5 and they are used in Method 3. Through the linear regression, the open circuit voltage and the Seebeck coefficient can be obtained in the form of Eq. (10) and the regressed equations are written as follows

$$V_{oc} = 0.3421 + 0.0479\Delta T \text{ (at low-temperature cooling condition, } T_w \cong 1^\circ\text{C)} \quad (13)$$

$$V_{oc} = 0.0069 + 0.0466\ T \quad \text{(at normal cooling condition, } T_w \cong 30^\circ\text{C)}. \quad (14)$$

It should be noted that there are two sets of experimental data from the two cooling conditions, so two Seebeck coefficients are obtained

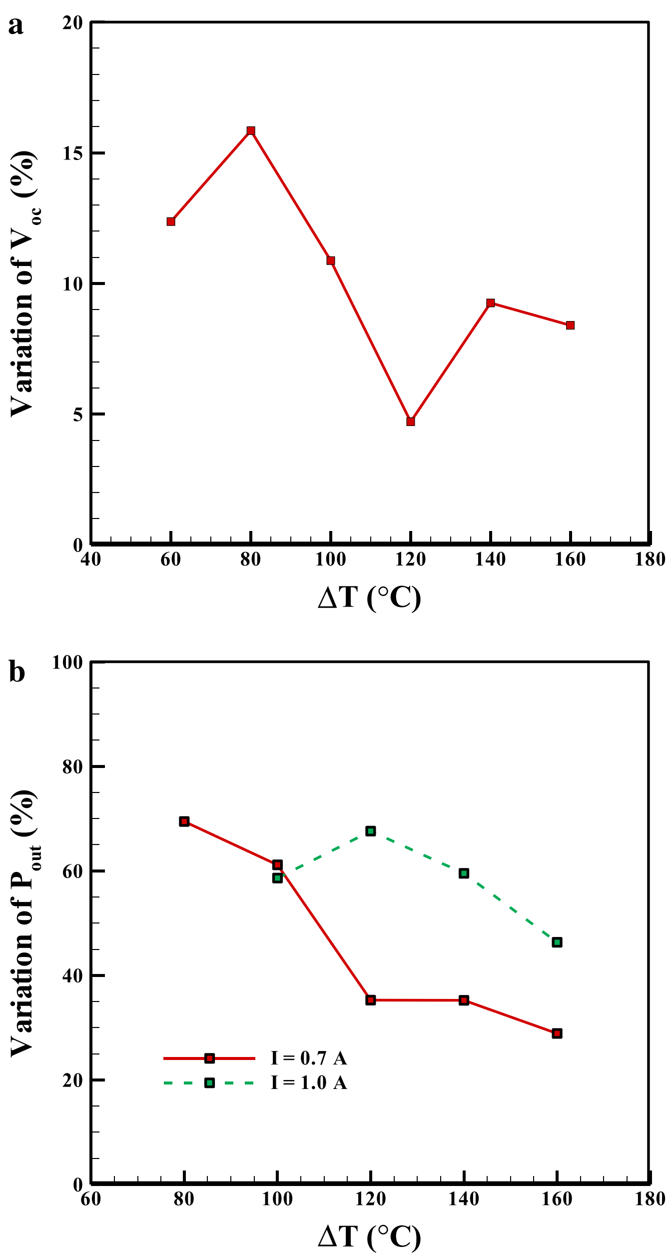

Fig. 7. Variations in percentage of (a) open circuit voltage and (b) output power versus temperature difference.

from Method 3 in terms of Eq. (11). The values of Seebeck coefficient at the low-temperature and normal cooling conditions are 1.887×10^{-4} and 1.835×10^{-4} V K^{-1}, respectively. Then, the output power can be predicted by Eq. (8) where the internal resistance is measured and its value is 3.54 Ω.

Error analysis of prediction

The predicted results of Seebeck coefficient from the three methods are plotted in Fig. 8. The Seebeck coefficient gotten from Method 1 is the highest, whereas it is the lowest from Method 3 at the normal cooling condition. The obtained Seebeck coefficient from Method 2 is lower than that from Method 1 but higher than that from Method 3. It should be pointed out that the Seebeck coefficient of Method 3 at the low-temperature cooling condition is higher than that at the normal one around 5.2 μV K^{-1}. This behavior is consistent with the observations in Fig. 6 where the performance of the TEC at the low-temperature cooling condition is better.

The predicted open circuit voltage based on the three methods are compared with the experimental data and shown in Fig. 9. As a whole, the predictions are close to the experimental results, regardless of which method is adopted. At present, the relative error of the predicted result is defined by

$$\text{Relative error } (\%) = \frac{\left|D_{\text{prediction}} - D_{\text{experiment}}\right|}{D_{\text{experiment}}} \times 100. \quad (15)$$

For the low-temperature cooling condition, the maximum relative errors of the open circuit voltage from Methods 1, 2, and 3 are 3.1, 8.6, and 2.0%, respectively, and the average relative errors from the three methods are 2.4, 5.2, and 1.1%, respectively, as listed in Table 2. For the case of normal cooling condition, the average errors in the open circuit voltage from the three methods are 9.7, 3.5, and 1.3%. With emphasis shifted to the output power, Fig. 10 depicts that the difference between the predictions and the experiments are not as good as those in Fig. 9. Specifically, with the condition of low-temperature cooling, the average errors of output power from Methods 1, 2, and 3 at $I =$ 0.7 A are 33.3, 29.1, 25.5%, respectively, and they are 56.7, 53.0, and 29.7% at $I = 1.0$ A (Table 2). For the case of normal cooling condition, the average errors of output power from the three methods at $I =$

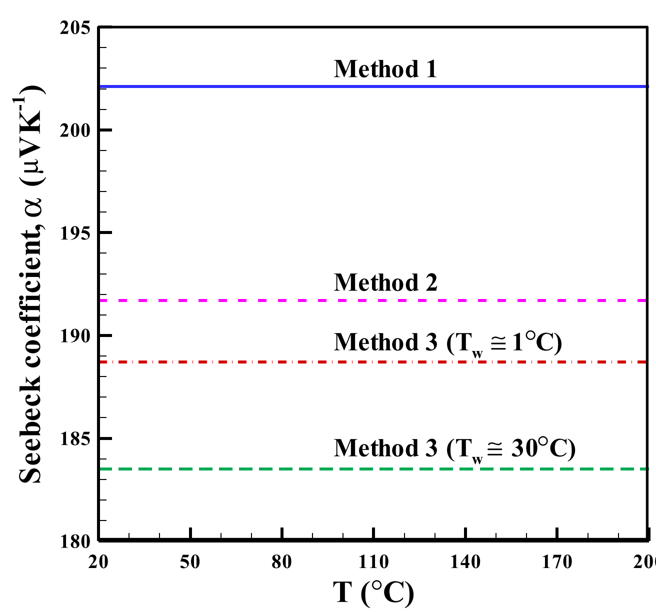

Fig. 8. Distributions of Seebeck coefficient predicted from three different methods.

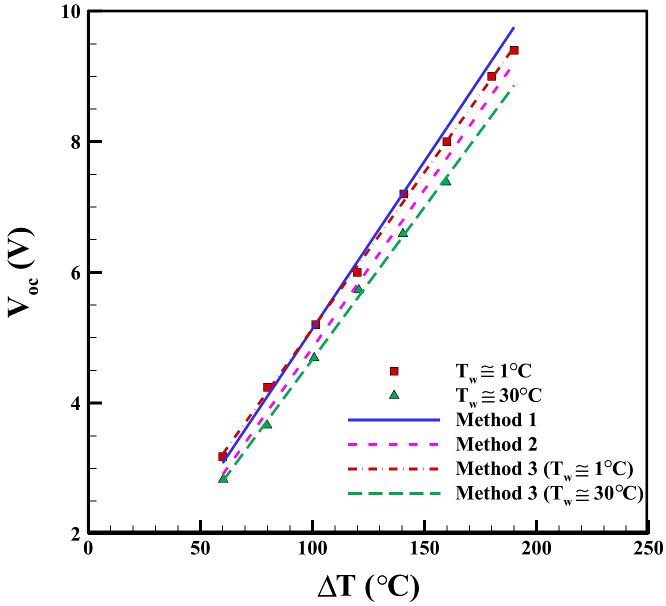

Fig. 9. Distributions of open circuit voltage from experiments and predictions.

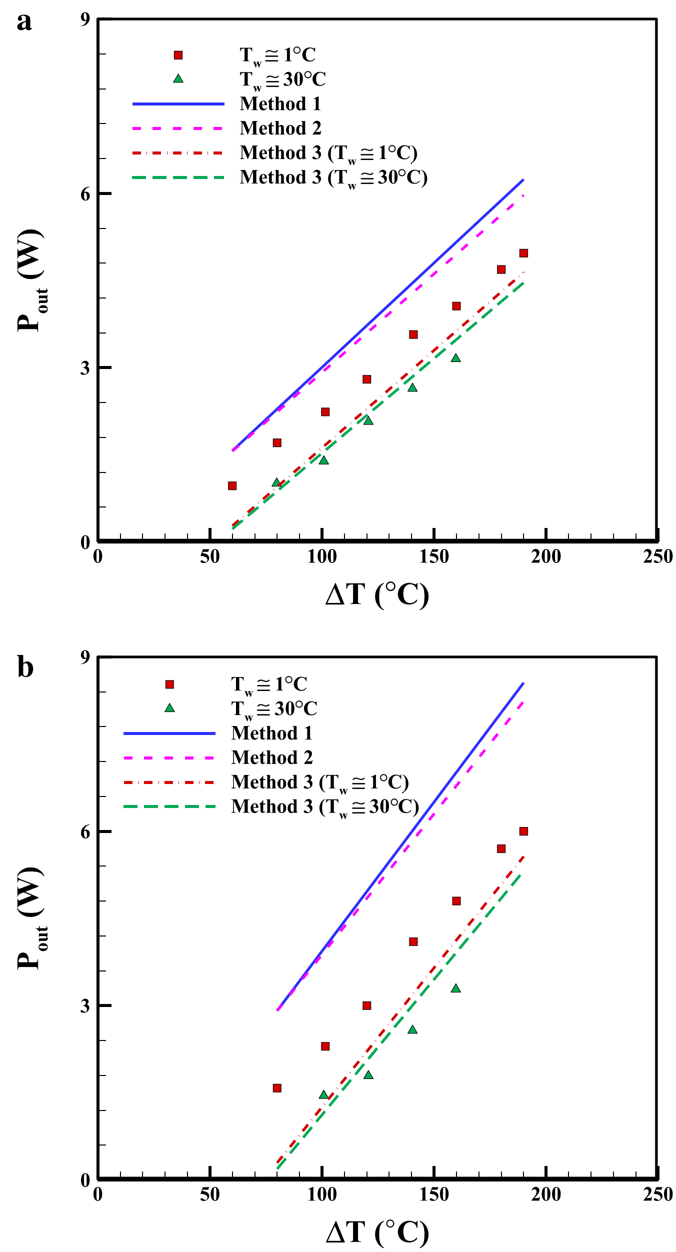

Fig. 10. Distributions of output power from experiments and predictions at (a) I = 0.7 A and (b) I = 1.0 A.

0.7 A are 91.1, 85.0, 9.3%, respectively, and they are 149.0, 142.9, and 18.3% at $I = 1.0$ A.

These results reveal that Method 3 gives the most precise predictions in the performance of the TEC. This arises from the fact that the predictions of Method 3 are based on the experimental measurements in part, whereas Methods 1 and 2 merely use the parameters which are provided in the datasheet at specified conditions. Table 2 also indicates that the relative errors of Method 1 and Method 2 in Fig. 9 are smaller than those in Fig. 10. Only one calculated property, the Seebeck coefficient, is used when the open circuit voltage is evaluated, as expressed in Eq. (7). Once the output power is predicted, two calculated properties, including the Seebeck coefficient and internal resistance, are required, as written in Eq. (8). The uncertainty of the prediction rises when the calculated properties increase. This is the reason that the predictions of the open circuit voltage have smaller relative errors compared with those of the output power.

It is worthy of note that the relative error of output power becomes more pronounced when the electric current is enlarged (Fig. 10). This is attributed to the Peltier effect which is not considered in the predictions. When the electric current increases, the influence of the Peltier effect on the performance of TEC tends to grow (Chen et al., 2012b; Zhu et al., 2011) and this makes the prediction more deviate from the experiment, especially for Methods 1 and 2 at the normal cooling condition and $I = 1.0$ A (Table 2). In summary, the three methods possess the merit of easy prediction in the performance of a TEC module without complicated mathematical operations or experimental equipment, but it is inappropriate to predict the output power of the TEC module using when the Peltier effect is significant.

Table 2
A list of average relative errors (%) of open circuit voltage and output power at two different cooling conditions.

Method	1	2	2
Open circuit voltage			
Low-temperature cooling	2.4	5.2	1.1
Normal cooling	9.7	3.5	1.3
Output power			
Low-temperature cooling			
I = 0.7 A	33.3	29.1	25.5
I = 1.0 A	56.7	53.0	29.7
Normal cooling			
I = 0.7 A	91.1	85.0	9.3
I = 1.0 A	149.0	142.9	18.3

Prediction of output power

Because the predictions of TEC performance from Method 3 is better than from the other two methods, the predictions of output power curve corresponding to varied electric current from Method 3 at the two different cooling conditions are displayed in Fig. 11 where three different temperature differences (ΔT = 80, 140, and 190 °C) are considered. For the low-temperature cooling condition, corresponding to the cases of ΔT = 80, 140, and 190 °C the maximum output powers are exhibited at the currents of 0.54, 0.94, and 1.28 A, respectively (Fig. 11a). Basically, the curves at the normal cooling condition (Fig. 11b) are very close to those at the low-temperature cooling condition. It should be addressed that the optimal currents for different temperature differences are easy to be obtained based on Method 3.

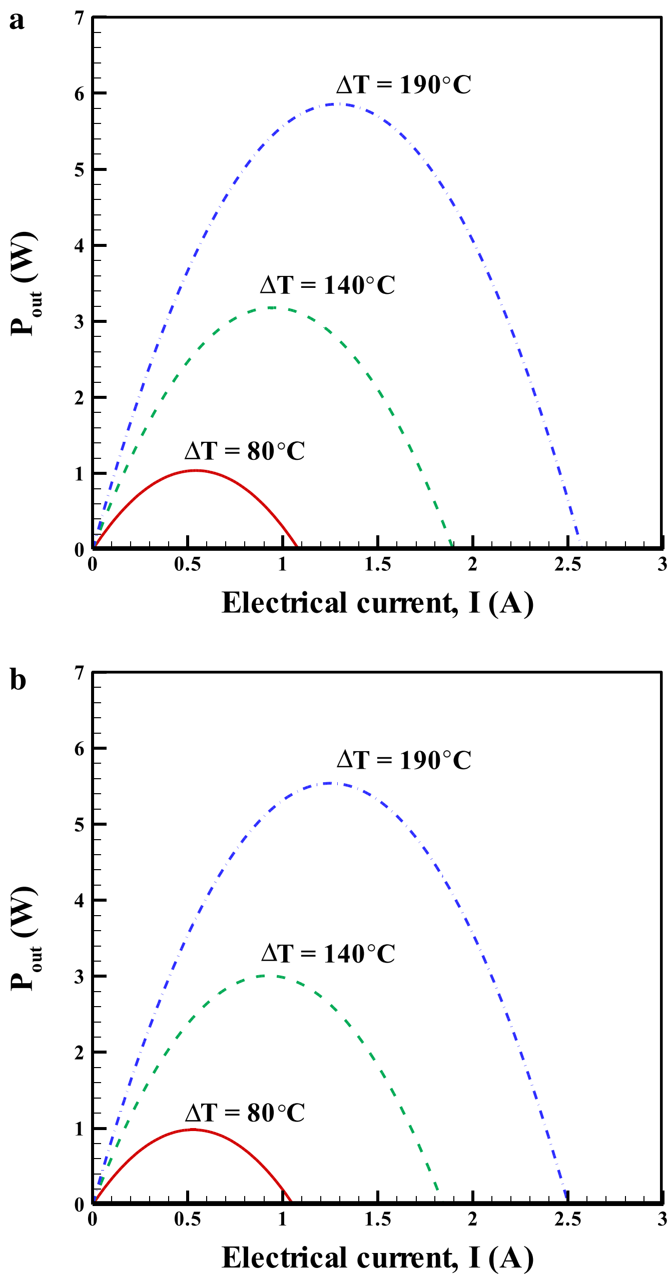

Fig. 11. Distributions of output power versus electric current at (a) the low-temperature cooling condition and (b) the normal cooling condition.

Therefore, the adopted methods are able to provide useful information in designing and constructing experiments for power generation from TEC modules.

Finally, a numerical method based on a finite element scheme (ANSYS v12.0.1) is carried out to simulate the power generation of the TEC module. The details of the numerical model can be found in a previous study (Wang et al., 2012b). The operating conditions of the numerical model are the same as those of the experiments and the material properties are obtained by Method 2. The predicted output power from Method 2 and the numerical simulation are displayed in Fig. 12. The isothermal contours along a TE pair under the conditions of low-temperature cooling, $\Delta T = 190$ °C, and $I = 1$ A are also demonstrated. The numerical simulations agree well with the theoretical data. However, the coolant temperature at a given ΔT plays no part in altering output power and it is different from the experimental results (Fig. 10). This is because the material properties used in Method 2 and the numerical

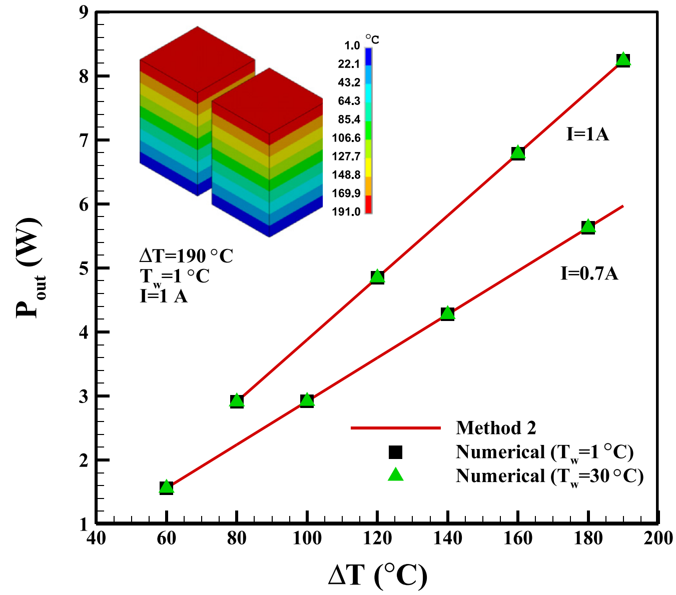

Fig. 12. Distributions of output power versus temperature difference from Method 2 and numerical simulations.

simulation are constant. In reality, they are inherently affected by temperature in a thermoelectric system.

Conclusions

An accurate prediction in the performance of TEC is conducive to the design of a power generation system through the thermoelectric effect. Three different methods have been employed to evaluate the performance of a TEC module for power generation. Two different cooling situations, including a low-temperature cooling operation and a normal cooling operation, are also regarded. From the experimental measurements, the TEC has a higher power generation at the low-temperature cooling condition than at the normal one and the improvement is over 5% under the same temperature difference. Accordingly, TECs are not only suitable for the low-temperature waste heat recovery but also for the operation at low-temperature cooling conditions. In Methods 1 and 2, the Seebeck coefficient and output power can be obtained directly from formulas without experimental measurements. They possess the merit of easy prediction, but the relative errors are higher since the temperature variation at the cold side of the TEC is not taken into account. With the aid of experimental data and the consideration of cooling temperature at the cold side, Method 3 gives the most accurate predictions in open circuit voltage and output power. Therefore, users who have simple instruments can make their selection of TEC more appropriate from Method 3. However, it is inappropriate to predict the performance using the three methods when the electric current is high to a certain extent, as a consequence of disregarding the Peltier effect. The optimal current corresponding to the maximum output power can also be obtained easily from the methods, so they can be applied for the design of the TEC system for power generation.

Acknowledgment

The authors acknowledge the financial support of the Ministry of Science and Technology, Taiwan, ROC, for this study.

References

Abramzon B. Numerical optimization of the thermoelectric cooling devices. ASME J. Electron Packag 2007;129:339–47.

Bell LE. Cooling, heating, generating power, and recovering waste heat with thermoelectric systems. Science 2008;321:1457–61.

Chen WH, Syu YJ. Thermal behavior and hydrogen production of methanol autothermal reforming with spiral preheating. Int J Hydrog Energy 2011;36:3397–408.

Chen WH, Chung YC, Liu JL. Analysis on energy consumption and performance of reheating furnace in a hot strip mill. Int Commun Heat Mass Transf 2005;32:695–706.

Chen WH, Liao CY, Hung CI. A numerical study on the performance of miniature thermoelectric cooler affected by Thomson effect. Appl Energy 2012a;89:464–73.

Chen WH, Liao CY, Hung CI, Huang WL. Experimental study on thermoelectric modules for power generation at various operating conditions. Energy 2012b;45:874–81.

Chen WH, Wang CC, Hung CI. Geometric effect on cooling power and performance of an integrated thermoelectric generation-cooling system. Energy Convers Manag 2014a;87:566–75.

Chen WH, Wang CC, Hung CI, Yang CC, Juang RC. Modeling and simulation for the design of thermal-concentrated solar thermoelectric generator. Energy 2014b;64:287–97.

Coleman HW, Steele Jr WG. Experimentation and uncertainty analysis for engineers. New York: Wiley; 1989.

Gurevich YG, Logvinov GN. Physics of thermoelectric cooling. Semicon Sci Technol 2005;20:R57–64.

Hsu CT, Huang GY, Chu HS, Yu B, Yao DJ. An effective Seebeck coefficient obtained by experimental results of a thermoelectric generator module. Appl Energy 2011;88:5173–9.

Huang BJ, Chin CJ, Duang CL. A design method of thermoelectric cooler. Int J Refrig 2000;23:208–18.

Huang MJ, Yen RH, Wang AB. The influence of the Thomson effect on the performance of a thermoelectric cooler. Int J Heat Mass Transf 2005;48:413–8.

Ioffe AF. Semiconductor thermoelements and thermoelectric cooling. 1st ed. London: Info-search Ltd.; 1957.

Kline SJ. The purpose of uncertainty analysis. ASME J Heat Transf 1985;117:153–60.

Luo Z. A simple method to estimate the physical characteristics of a thermoelectric cooler from vendor datasheets. Electron Cooling 2008;14:22–7.

Mahan GD. Figure of merit for thermoelectric. J Appl Phys 1989;65:1578–83.

Maneewan S, Chindaruksa S. Thermoelectric power generation system using waste heat from biomass drying. J Electron Mater 2009;38:974–80.

Martinez A, Astrain D, Rodriguez A. Experimental and analytical study on thermoelectric self cooling of devices. Energy 2011;36:5250–60.

Meng JM, Zhang XX, Wang XD. Dynamic response characteristics of thermoelectric generator predicted by a three-dimensional heat-electricity coupled model. J Power Sources 2014a;245:262–9.

Meng JM, Zhang XX, Wang XD. Multi-objective and multi-parameter optimization of a thermoelectric generator module. Energy 2014b;71:437–76.

Meng JH, Zhang XX, Wang XD. Characteristics analysis and parametric study of a thermoelectric generator by considering variable material properties and heat losses. Int J Heat Mass Transf 2015;80:227–35.

Min G, Rowe DM. Evaluation of thermoelectric modules for power generation. J Power Sources 1998;73:193–8.

Palacios P, Arenas A, Pecharroman RR, Pagola FL. Analytical procedure to obtain internal parameters from performance curves of commercial thermoelectric modules. Appl Therm Eng 2009;29:3501–5.

Riffat SB, Ma X. Thermoelectrics: a review of present and potential applications. Appl Therm Eng 2003;23:913–35.

Simons RE, Ellsworth MJ, Chu RC. An assessment of module cooling enhancement with thermoelectric coolers. ASME J Heat Transf 2005;127:76–84.

Wang XD, Huang YX, Cheng CH, Lin DTW, Kang CH. A three-dimensional numerical modeling of thermoelectric device with consideration of coupling of temperature field and electric potential field. Energy 2012a;47:488–97.

Wang CC, Hung CI, Chen WH. Design of heat sink for improving the performance of thermoelectric generator using a two-stage optimization. Energy 2012b;39:236–45.

Wang XD, Wang QH, Xu JL. Performance analysis of two-stage TECs (thermoelectric coolers) using a three-dimensional heat-electricity coupled model. Energy 2014;65:419–29.

Woo BC, Lee HW. Relation between electric power and temperature difference for thermoelectric generator. Int J Mod Phys B 2003;17:1421–6.

Wu KH, Hung CI. Thickness scaling characterization of thermoelectric module for small-scale electronic cooling. J Chin Soc Mech Eng 2009;30:475–81.

Zhu J, Gao J, Chen M, Zhang J, Du Q, Rosendahl LA, et al. Experimental study of a thermoelectric generating system. J Electron Mater 2011;40:744–52.